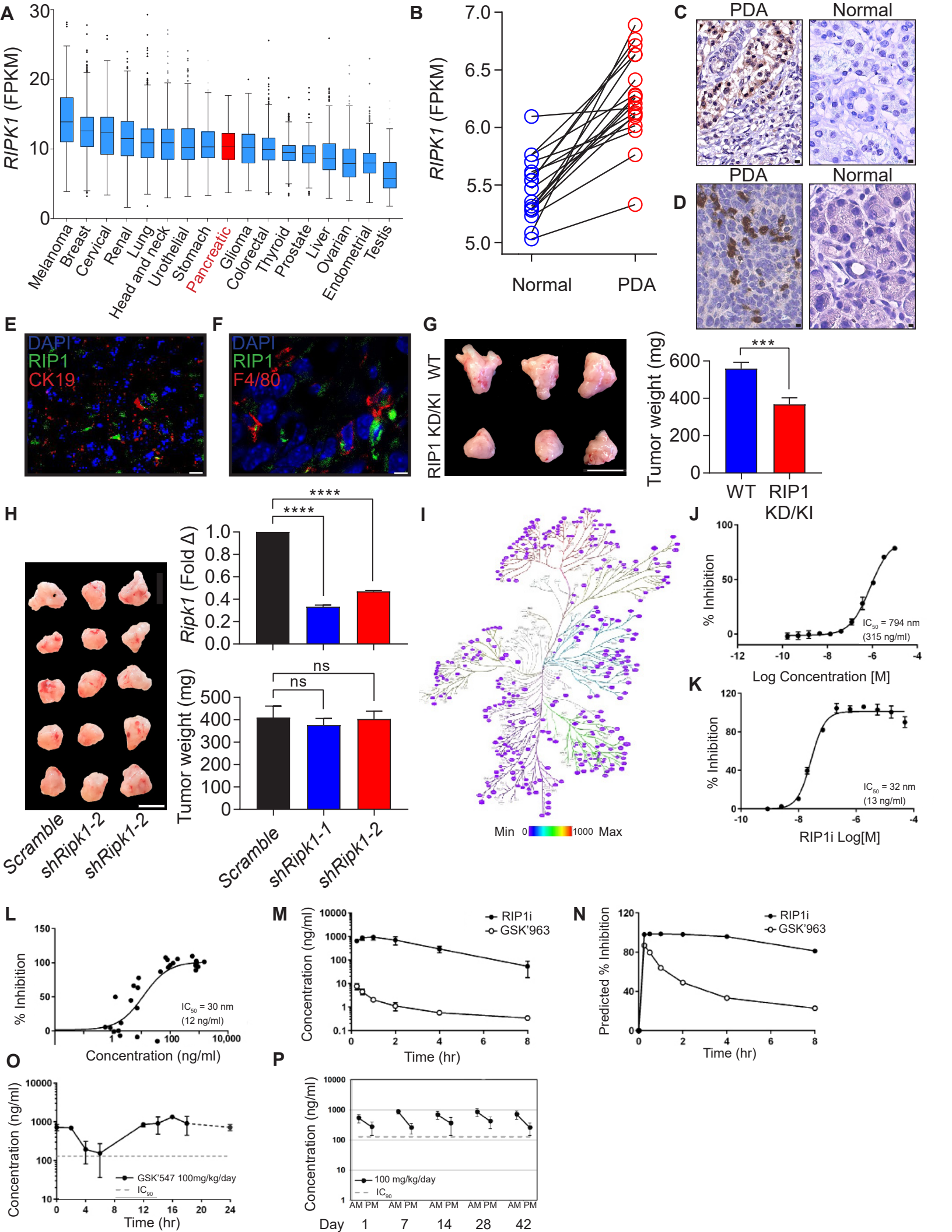
A
RIPK1 (FPKM)
Melanoma
Breast
Cervical
Renal
Lung
Head and neck
Urothelial
Stomach
Pancreatic
Glioma
Colorectal
Thyroid
Prostate
Liver
Ovarian
Endometrial
Testis
B
RIPK1 (FPKM)
Normal
PDA
C
PDA
Normal
D
PDA
Normal
E
DAPI
RIP1
CK19
F
DAPI
RIP1
F4/80
G
WT
RIP1 KD/KI
Tumor weight (mg)
***
WT
RIP1 KD/KI
H
Ripk1 (Fold Δ)
****
****
Tumor weight (mg)
ns
ns
Scramble
shRipk1-2
shRipk1-2
Scramble
shRipk1-1
shRipk1-2
I
Min 0
1000 Max
J
% Inhibition
IC50 = 794 nm
(315 ng/ml)
Log Concentration [M]
K
% Inhibition
IC50 = 32 nm
(13 ng/ml)
RIP1i Log[M]
L
% Inhibition
IC50 = 30 nm
(12 ng/ml)
Concentration (ng/ml)
M
Concentration (ng/ml)
RIP1i
GSK'963
Time (hr)
N
Predicted % Inhibition
RIP1i
GSK'963
Time (hr)
O
Concentration (ng/ml)
GSK'547 100mg/kg/day
IC90
Time (hr)
P
Concentration (ng/ml)
100 mg/kg/day
IC90
AM PM AM PM AM PM AM PM AM PM
Day 1 7 14 28 42

Figure S1, related to Figure 1: RIP1 is highly expressed in PDA and can be targeted *in vivo* by a small molecule inhibitor. (A) Comparison of *RIPK1* expression in various cancer types based on data from TCGA. Boxes in boxplot indicate the interquartile range (IQR) or central 50% of the FPKM values mined from the TCGA-based bulk tumor RNAseq within each cancer type. The central line within each box indicates the median FPKM value and the whiskers extend to the most extreme data points that fall within the 1.5x IQR range. **(B)** Comparison of *RIPK1* expression in PDA vs adjacent benign pancreatic tissue in matched patient samples based on data from TCGA. **(C, D)** Paraffin-embedded sections of human (C) and murine **(D)** PDA tumors and adjacent normal pancreata were tested for expression of RIP1. Representative images are shown (scale bars = 10 μm). **(E)** Frozen sections of orthotopic KPC tumors were tested for co-expression of RIP1 and CK19 (scale bar = 1 μm). **(F)** Frozen sections of orthotopic KPC tumors were tested for co-expression of RIP1 and F4/80 (scale bar = 1 μm). **(G)** Representative images (scale bar = 1 cm) and tumor weights of orthotopic KPC tumors in WT and RIP1 KD/KI mice sacrificed on day 21 (n=10/group). This experiment was repeated three times with similar results (***$p<0.001$). **(H)** Representative images (scale bar = 1 cm) and day 21 weights of KPC tumors in WT mice administered orthotopic tumors cells treated with either shRNA directed against *Ripk1* or control scrambled shRNA (n=5/group). The efficacy of *Ripk1* knockdown was measured by qPCR. This experiment was repeated twice with similar results using separate shRNA vectors (****$p<0.0001$). **(I)** Kinase selectivity plot for RIP1i evaluated against 371 kinases assayed at 10 μM in duplicate. Compound selectivity is represented in a dendrogram view of the human kinome phylogenetic tree. Blue circles indicate kinase inactivity. **(J)** A fluorescent polarization (FP) binding assay was used to quantitate the interaction of RIP1i at the ATP-binding pocket of RIP1 by competition with a fluorescently labeled ATP-competitive ligand. Dose–response curve for RIP1i evaluating the

affinity of compound for RIP1. The graph represents combined data from two independent experiments. **(K)** Activity of RIP1i *in vitro* was evaluated by measuring cellular viability in L929 cells after treatment with TNFα and zVAD. Combined data from two independent experiments are shown (n=3). **(L)** Activity of RIP1i *in vivo* was evaluated in TNF+zVAD-induced shock. Inhibition of temperature loss in this model was evaluated in a dose response manner. Combined results of seven animals per group are shown. **(M)** Pharmacokinetic profiles of RIP1i and GSK'963 in WT mice (10 mg/kg and 20 mg/kg, respectively; n=3/group). **(N)** Modeling of predicted % inhibition against RIP1 using the observed pharmacokinetic profiles of RIP1i and GSK'963 and their potencies in inhibiting TNF+zVAD-induced cell death in L929 cells. **(O)** Steady state pharmacokinetic profile over 24 hr of RIP1i dosed in chow at ~100 mg/kg/day in C57BL/6 mice. The data represent the combined results of two animals. The 24 hr time point is extrapolated with the assumption that the profile returns to 0 hr time point levels. This is indicated by the dotted line from the 18-24 hr timepoints. **(P)** Drug levels of RIP1i over time in WT mice (~100 mg/kg/day, in chow). Samples were collected in the morning (7AM) and afternoon (4PM) on the indicated days (n=10 mice/data point). Data are displayed as average ± SEM.

Table S1, related to Figure 1: Kinase Panel Profile for GSK'547 (RIP1i).[a]

RBC Gene Name	GSK'547A (10 μM) Average % Inhibition	RBC Gene Name	GSK'547A (10 μM) Average % Inhibition	RBC Gene Name	GSK'547A (10 μM) Average % Inhibition
ABL1	7.73	FES/FPS	-3.62	PAK3	-6.79
ABL2/ARG	3.04	FGFR1	2.72	PAK4	-7.17
ACK1	21.63	FGFR2	1.17	PAK5	-2.77
AKT1	3.32	FGFR3	0.78	PAK6	-0.21
AKT2	3.97	FGFR4	1.83	PASK	1.22
AKT3	1.41	FGR	5.66	PBK/TOPK	-5.75
ALK	20.79	FLT1-VEGFR1	4.12	PDGFRa	-0.79
ALK1/ACVRL1	13.96	FLT3	0.82	PDGFRb	6.59
ALK2/ACVR1	-4.90	FLT4-VEGFR3	-2.05	PDK1/PDPK1	-1.05
ALK3/BMPR1A	-8.95	FMS	5.03	PEAK1	6.45
ALK4/ACVR1B	-2.57	FRK-PTK5	0.71	PHKg1	9.78
ALK5/TGFBR1	-2.25	FYN	-4.16	PHKg2	-4.43
ALK6/BMPR1B	0.01	GCK/MAP4K2	1.92	PIM1	4.22
ARAF	9.18	GLK/MAP4K3	-9.35	PIM2	-2.18
ARK5/NUAK1	0.60	GRK1	-18.92	PIM3	-3.61
ASK1/MAP3K5	0.34	GRK2	-0.54	PKA	5.63
Aurora A	-0.96	GRK3	-6.24	PKAcb	4.63
Aurora B	19.48	GRK4	-4.48	PKAcg	8.87
Aurora C	4.33	GRK5	-9.96	PKCa	5.63
AXL	5.95	GRK6	-5.80	PKCb1	-6.63
BLK	7.06	GRK7	5.06	PKCb2	4.65
BMPR2	-5.88	GSK3a	3.47	PKCd	6.98
BMX/ETK	0.07	GSK3b	-1.83	PKCepsilon	0.51
BRAF	4.16	Haspin	1.18	PKCeta	12.07
BRK	8.14	HCK	-8.65	PKCg	6.16
BRSK1	3.75	HGK/MAP4K4	-3.64	PKCiota	0.82
BRSK2	-0.31	HIPK1	-2.81	PKCmu/PRKD1	3.81
BTK	13.46	HIPK2	-3.74	PKCnu/PRKD3	4.61
c-Kit	4.51	HIPK3	-12.20	PKCtheta	-5.93
c-MER	4.74	HIPK4	3.22	PKCzeta	-5.55
c-MET	-6.00	HPK1/MAP4K1	-29.59	PKD2/PRKD2	9.46
c-Src	-3.96	IGF-1R	-4.15	PKG1a	4.28
CAMK1a	6.57	IKKa/CHUK	0.56	PKG1b	6.38
CAMK1b	2.91	IKKb/IKBKB	4.74	PKG2/PRKG2	11.61
CAMK1d	4.21	IKKe/IKBKE	4.94	PKN1/PRK1	6.91
CAMK1g	1.16	IR	-1.02	PKN2/PRK2	6.39
CAMK2a	-4.21	IRAK1	-5.21	PKN3/PRK3	12.84
CAMK2b	7.32	IRAK4	17.27	PLK1	-1.17
CAMK2d	-5.47	IRR/INSRR	16.59	PLK2	3.24
CAMK2g	7.71	ITK	1.94	PLK3	7.26
CAMK4	-2.27	JAK1	0.11	PLK4/SAK	5.81
CAMKK1	9.24	JAK2	0.06	PRKX	0.66
CAMKK2	5.58	JAK3	2.91	PYK2/FAK2	-1.47
CDC7/DBF4	-5.33	JNK1	-3.82	RAF1	9.39
CDK1/cyclin A	-3.35	JNK2	-2.67	RET	-7.23
CDK1/cyclin B	4.88	JNK3	3.38	RIPK2	4.52
CDK1/cyclin E	10.10	KDR/VEGFR2	7.82	RIPK3	-4.18
CDK14/cyclin Y (PFTK1)	-3.33	KHS/MAP4K5	11.68	RIPK4	5.16
CDK16/cyclin Y (PCTAIRE)	8.74	KSR1	3.57	RIPK5	29.58
CDK17/cyclin Y (PCTK2)	-2.03	KSR2	0.18	ROCK1	4.52
CDK18/cyclin Y (PCTK3)	-29.77	LATS1	-9.77	ROCK2	5.57
CDK19/cyclin C	-3.46	LATS2	11.51	RON/MST1R	2.47
CDK2/cyclin A	-1.04	LCK	11.22	ROS/ROS1	0.28
CDK2/Cyclin A1	8.48	LCK2/ICK	2.88	RSK1	5.79
CDK2/cyclin E	0.46	LIMK1	6.54	RSK2	6.58
CDK2/cyclin E2	-4.58	LIMK2	7.60	RSK3	-18.98
CDK2/cyclin O	6.68	LKB1	-17.29	RSK4	5.04
CDK3/cyclin E	-1.55	LOK/STK10	-5.59	SBK1	-3.22
CDK3/cyclin E2	-3.63	LRRK2	5.32	SGK1	5.95
CDK4-cyclin D1	-0.46	LYN	5.54	SGK2	11.06
CDK4-cyclin D3	2.52	LYN B	0.76	SGK3/SGKL	-1.36
CDK5/p25	19.38	MAK	-2.40	SIK1	-5.56

CDK5/p35	5.10	MAPKAPK2	6.58	SIK2	1.30
CDK6-cyclin D1	5.10	MAPKAPK3	-11.93	SIK3	1.55
CDK6-cyclin D3	16.02	MAPKAPK5/PRAK	1.54	SLK/STK2	-0.19
CDK7/cyclin H	-1.40	MARK1	-0.52	SNARK/NUAK2	9.41
CDK9-cyclin K	6.94	MARK2/PAR-1Ba	1.28	SNRK	0.13
CDK9/cyclin T1	-9.75	MARK3	-9.43	SRMS	-6.77
CDK9/cyclin T2	-0.93	MARK4	4.08	SRPK1	5.64
CHK1	1.41	MEK1	0.30	SRPK2	-4.72
CHK2	10.16	MEK2	-3.78	SSTK/TSSK6	0.15
CK1a1	-3.19	MEK3	-13.42	STK16	-13.48
CK1a1L	7.76	MEK5	3.46	STK21/CIT	2.84
CK1d	0.48	MEKK1	15.45	STK22D/TSSK1	-1.92
CK1epsilon	-12.84	MEKK2	-11.59	STK25/YSK1	10.92
CK1g1	11.01	MEKK3	16.41	STK32B/YANK2	21.93
CK1g2	9.97	MEKK6	-1.49	STK32C/YANK3	-11.87
CK1g3	0.35	MELK	15.07	STK33	-16.33
CK2a	21.17	MINK/MINK1	1.85	STK38-NDR1	-1.64
CK2a2	21.30	MKK4	0.47	STK38L/NDR2	3.95
CLK1	-1.23	MKK6	0.64	STK39/STLK3	-4.72
CLK2	3.21	MKK7	2.13	SYK	-33.59
CLK3	4.64	MLCK/MYLK	9.36	TAK1	2.49
CLK4	4.14	MLCK2/MYLK2	12.93	TAOK1	-0.37
COT1/MAP3K8	-0.65	MLK1/MAP3K9	6.41	TAOK2-TAO1	4.23
CSK	17.05	MLK2/MAP3K10	20.62	TAOK3-JIK	6.15
CTK-MATK	8.85	MLK3/MAP3K11	-11.20	TBK1	13.32
DAPK1	-7.56	MLK4	5.79	TEC	3.22
DAPK2	5.49	MNK1	10.63	TESK1	-7.67
DCAMKL1	0.41	MNK2	4.37	TESK2	0.07
DCAMKL2	-0.58	MRCKa/CDC42BPA	5.11	TGFBR2	-0.89
DDR1	-8.41	MRCKb/CDC42BPB	10.73	TIE2/TEK	0.09
DDR2	1.83	MSK1/RPS6KA5	4.79	TLK1	6.70
DLK/MAP3K12	23.58	MSK2/RPS6KA4	-1.80	TLK2	6.83
DMPK	11.43	MSSK1-STK23	-4.06	TNIK	4.36
DMPK2	6.65	MST1/STK4	5.22	TNK1	-3.80
DRAK1/STK17A	1.13	MST2/STK3	-2.37	TRKA/NTRK1	32.92
DYRK1/DYRK1A	1.94	MST3/STK24	4.09	TRKB	3.27
DYRK1B	5.96	MST4	15.31	TRKC	-0.96
DYRK2	-0.21	MUSK	4.24	TSSK2	3.95
DYRK3	11.92	MYLK3	-6.57	TSSK3/STK22C	-6.26
DYRK4	-8.86	MYLK4	3.54	TTBK1	3.41
EGFR	11.00	MYO3A	5.26	TTBK2	-2.07
EPHA1	4.96	MYO3b	6.66	TXK	2.88
EPHA2	-1.88	NEK1	9.46	TYK1/LTK	15.83
EPHA3	7.56	NEK11	-1.63	TYK2	0.81
EPHA4	-4.46	NEK2	-6.16	TYRO3-SKY	-1.40
EPHA5	-2.34	NEK3	-1.86	ULK1	8.22
EPHA6	6.22	NEK4	-10.65	ULK2	7.05
EPHA7	4.02	NEK5	12.21	ULK3	5.79
EPHA8	5.16	NEK6	-1.40	VRK1	-3.21
EPHB1	-8.68	NEK7	-0.95	VRK2	-2.28
EPHB2	2.88	NEK8	-0.20	WEE1	0.45
EPHB3	-1.48	NEK9	1.94	WNK1	-6.74
EPHB4	16.08	NIM1	-1.43	WNK2	6.65
ERBB2/HER2	-8.66	NLK	7.81	WNK3	10.78
ERBB4/HER4	-1.32	OSR1/OXSR1	0.79	YES/YES1	15.97
ERK1	-11.25	P38a/MAPK14	-3.38	YSK4/MAP3K19	0.18
ERK2/MAPK1	-0.44	P38b/MAPK11	-3.16	ZAK/MLTK	-2.37
ERK5/MAPK7	3.23	P38d/MAPK13	9.32	ZAP70	4.99
ERK7/MAPK15	8.65	P38g	-14.76	ZIPK/DAPK3	-7.35
ERN1/IRE1	1.43	p70S6K/RPS6KB1	-2.85	**# of Kinases >/= 50% Inhib.**	0
ERN2/IRE2	1.18	p70S6Kb-RPS6KB2	1.30	**# of Kinases >/= 70% Inhib.**	0
FAK/PTK2	4.73	PAK1	-5.51	**# of Kinases >/= 90% Inhib.**	0
FER	0.39	PAK2	1.64		

[a]GSK'547 was tested at 10 μM concentration in duplicate against 371 kinases in the Reaction Biology Corporation kinase panel. Control compound was tested in 10-dose IC50 mode with 3-fold serial dilution starting at 20 μM. Reactions were carried out at 10 μM ATP concentration. Full protocol details are available at http://www.reactionbiology.com. Data is reported as % enzyme inhibition (relative to DMSO controls) in the table below. The kinase panel did not include RIP1 kinase. No inhibition >33% (average of n =2) was observed at 10 μM concentration.

Table S2, related to Figure 1: Comparison of pharmacokinetic features of RIP1i vs Nec-1s

	RIP1i	**Nec-1s**
Mouse L929 cell IC_{50}[a]	32 nM	890 nM
Target Conc (L929 ~IC_{90})	320 nM	8900 nM
Concentration after 22-24 hrs	1840 nM[b]	237 nM[c]

[a]Mouse L-cell NCTC 929 (L929) cellular potency was obtained as described previously (Harris, P. A. et al, J. Med. Chem. 2016) for RIP1i (n=2) and Nec-1s (n= 98).
[b]RIP1i was administered to mice in food and then blood levels were sampled in the morning 22 hr after beginning diet.
[c]Nec-1s was administered to mice in drinking water (0.5 mg/mL) and plasma levels sampled in the morning at 24 hr as described (Ofengeim, P. et al, Cell Rep. 2015).

Table S3, related to Figure 1: Pathology report of 8 week tolerability study with GSK'547 dosed in chow.[a]

	Male		Female	
	Control	100 mg/kg/day	Control	100 mg/kg/day
Number of animals	5	5	5	5
BRAIN				
Examined	5	5	5	5
No Abnormality detected	5	5	5	5
CEACUM				
Examined	5	5	5	5
No Abnormality detected	5	5	5	5
COLON				
Examined	5	5	5	5
No Abnormality detected	5	5	5	5
DUODENUM				
Examined	5	5	5	5
No Abnormality detected	5	5	5	5
EYES				
Examined	5	5	5	5
No Abnormality detected	5	5	5	5
HEART				
Examined	5	5	5	5
No Abnormality detected	5	4	5	5
Mineralisation; focal, myocardium	0	1	0	0
minimal	0	1	0	0
ILEUM				
Examined	5	5	5	5
No Abnormality detected	5	5	5	5
JEJUNUM				
Examined	5	5	5	5
No Abnormality detected	5	5	5	5
KIDNEYS				
Examined	5	5	5	5
No Abnormality detected	5	5	5	5
LIVER				
Examined	5	5	5	5
No Abnormality detected	5	5	4	5
Necrosis; focal, hepatocyte; subcapsular	0	0	1	0
minimal	0	0	1	0

	Male		Female	
	Control	100 mg/kg/day	Control	100 mg/kg/day
Number of animals	5	5	5	5
LUNG				
Examined	5	5	5	5
No Abnormality detected	4	5	4	5
Haemorrhage; alveolus	0	0	1	0
minimal	0	0	1	0
Inflammatory cell infiltrate; mononuclear cell, perivascular	1	0	0	0
minimal	1	0	0	0
LYMPH NODE - INGUINAL				
Examined	5	5	5	5
No Abnormality detected	4	5	5	5
Celularity increased	1	0	0	0
marked	1	0	0	0
LYMPH NODE - MESENTERIC				
Examined	5	5	5	4
No Abnormality detected	5	5	5	4
Not Examined: No Section	0	0	0	1
OPTIC NERVE				
Examined	4	4	5	4
No Abnormality detected	4	4	5	4
Not Examined: Insufficient Tissue to Evaluate	1	1	0	1
PANCREAS				
Examined	5	5	5	5
No Abnormality detected	5	5	5	5
SPINAL CORD				
Examined	5	5	5	5
No Abnormality detected	5	5	5	5
SPLEEN				
Examined	5	5	5	5
No Abnormality detected	5	5	5	5
STOMACH				
Examined	5	5	5	5
No Abnormality detected	5	5	5	5

[a]GSK'547 was dosed in chow at 100 mg/kg/day in C57Bl/6 mice for 8 weeks (n = 5 males and 5 females). After 8 weeks, the indicated organs were collected and processed for histopathological assessment.

Table S4, related to Figure 1: X-ray diffraction processing and refinement statistics for the RIP1 GSK'547 complex structure.

	Overall	**Innershell**	**Outershell**
Low Res Limit (Å)	80.65	80.65	3.49
High Res Limit (Å)	3.49	8.55	3.49
Rmerge (all)	0.131	0.051	0.639
Mean(I/σI)	7.7	21.2	2.5
Observations (unique)	46855 (8924)	3240 (647)	10781 (2087)
Completeness	97.7	94.4	97.0
Multiplicity	5.3	5.0	5.2
Space Group	P212121		
Unit Cell Dimensions	102.649 130.370 50.839 90.00 90.00 90.00		
R-factor (R-Free)	0.2084 (0.2270)		

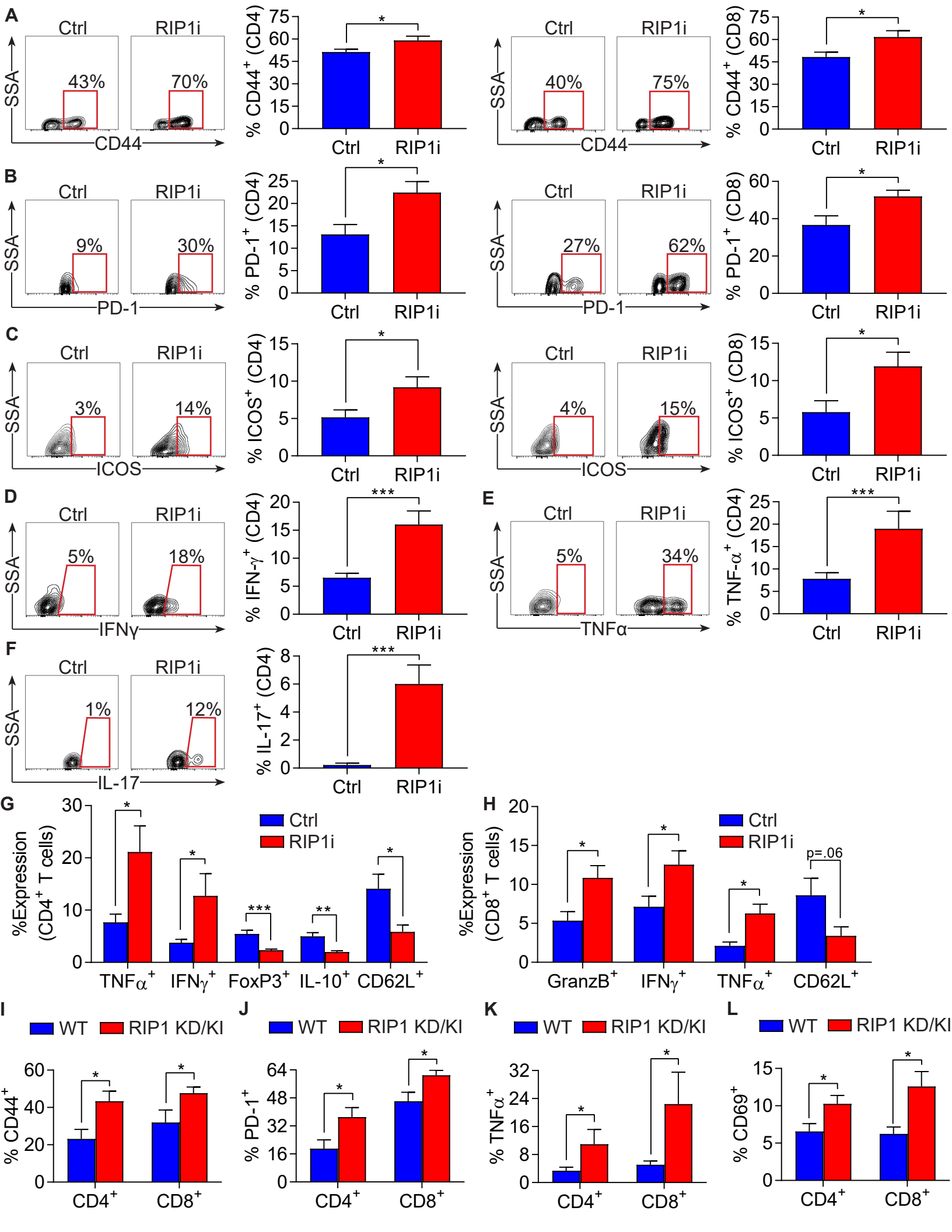
A
Ctrl
RIP1i
SSA
43%
70%
CD44
% CD44+ (CD4)
Ctrl
RIP1i
40%
75%
CD44
% CD44+ (CD8)
B
9%
30%
PD-1
% PD-1+ (CD4)
27%
62%
PD-1
% PD-1+ (CD8)
C
3%
14%
ICOS
% ICOS+ (CD4)
4%
15%
ICOS
% ICOS+ (CD8)
D
5%
18%
IFNγ
% IFN-γ+ (CD4)
E
5%
34%
TNFα
% TNF-α+ (CD4)
F
1%
12%
IL-17
% IL-17+ (CD4)
G
%Expression (CD4+ T cells)
TNFα+
IFNγ+
FoxP3+
IL-10+
CD62L+
H
%Expression (CD8+ T cells)
GranzB+
IFNγ+
TNFα+
CD62L+
p=.06
I
WT
RIP1 KD/KI
% CD44+
CD4+
CD8+
J
% PD-1+
K
% TNFα+
L
% CD69+

Figure S2, related to Figure 2: Targeting RIP1 leads to high activation of T cells infiltrating PDA in multiple models. (A-F) WT mice bearing KPC liver metastases were treated with RIP1i or control and were sacrificed at 21 days (n=10/group). $CD4^+$ and $CD8^+$ T cells were tested for expression of CD44 (A), PD-1 **(B)**, and ICOS **(C)** by flow cytometry. $CD4^+$ T cells were additionally analyzed for expression of IFNγ **(D)**, TNFα **(E)**, and IL-17 **(F)**. This experiment was repeated twice. (**G, H**) WT mice bearing orthotopic KPC tumors were treated with RIP1i or control starting at day 10 and were sacrificed at day 21 (n=10/group). $CD4^+$ (G) and $CD8^+$ **(H)** T cells were assayed for activation by flow cytometry. This experiment was repeated twice. **(I-L)** WT and RIP1 KD/KI mice bearing orthotopic KPC tumors were sacrificed at day 21 (n=10/group). $CD4^+$ and $CD8^+$ T cells were assayed for expression of CD44 (I), PD-1 **(J)**, TNFα **(K)**, and CD69 **(L)**. This experiment was repeated 3 times with similar results. Data are displayed as average ± SEM (*p<0.05; **p<0.01; ***p<0.001).

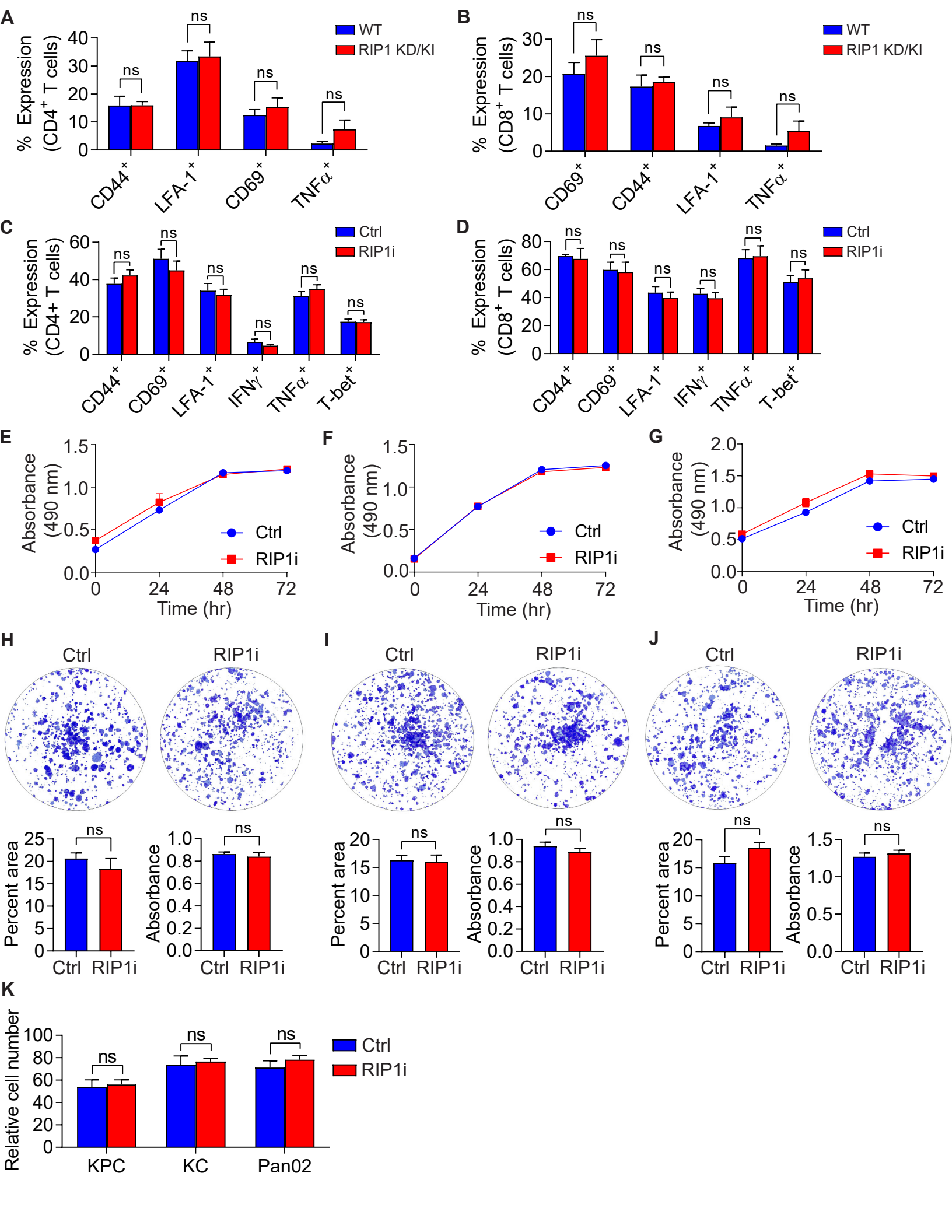
A
% Expression (CD4+ T cells)
WT
RIP1 KD/KI
ns
CD44+
LFA-1+
CD69+
TNFα+
B
% Expression (CD8+ T cells)
C
% Expression (CD4+ T cells)
Ctrl
RIP1i
IFNγ+
T-bet+
D
% Expression (CD8+ T cells)
E
Absorbance (490 nm)
Time (hr)
F
G
H
Ctrl
RIP1i
Percent area
Absorbance
I
J
K
Relative cell number
KPC
KC
Pan02

Figure S3, related to Figure 3: RIP1i does not directly induce changes in the phenotype of T cells or tumor cells. (A, B) Splenic $CD4^+$ (A) and $CD8^+$ **(B)** T cell phenotype was compared in untreated WT and RIP1 KD/KI mice (n=6/group). **(C, D)** Polyclonal $CD4^+$ (C) and $CD8^+$ **(D)** splenic T cells were activated by CD3/CD28 co-ligation in the presence of RIP1i or vehicle and tested for expression of activation markers at 72 hr. **(E-G)** *In vitro* cellular proliferation was measured using the XTT assay in KPC-derived tumor cells (E), KC-derived epithelial cells **(F)**, and Pan02 cells **(G)** treated with RIP1i or vehicle. **(H-J)** Colony formation was determined in RIP1i- or vehicle-treated KPC-derived tumor cells (H), KC-derived epithelial cells **(I)**, and Pan02 cells **(J)**. **(K)** Cellular migration was measured in RIP1i- or vehicle-treated KPC-derived tumor cells, KC-derived epithelial cells, and Pan02 cells. All *in vitro* experiments were performed in quadruplicate and repeated at least twice. Data are displayed as average ± SEM.

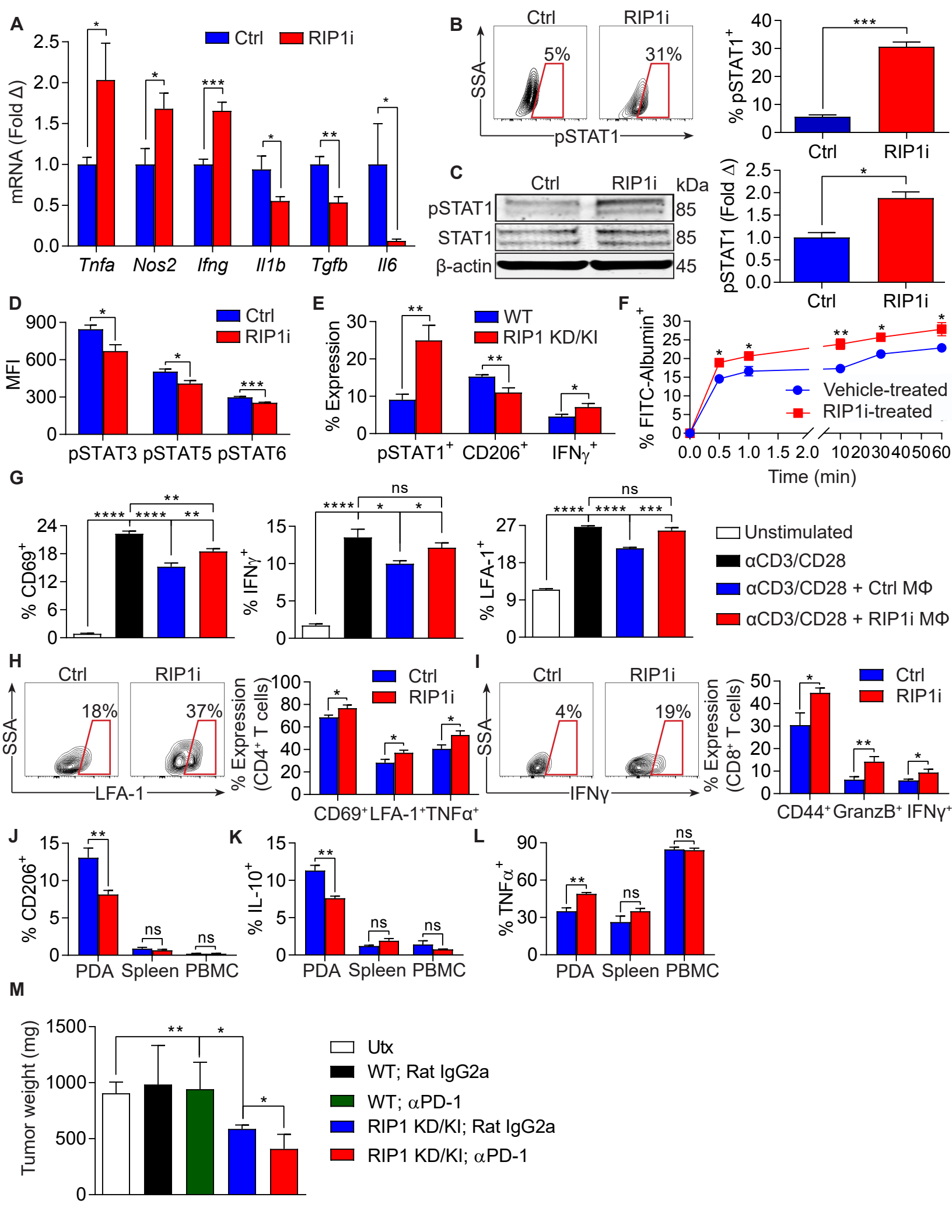
A
Ctrl
RIP1i
mRNA (Fold Δ)
Tnfa
Nos2
Ifng
Il1b
Tgfb
Il6
B
Ctrl
RIP1i
5%
31%
SSA
pSTAT1
% pSTAT1+
C
Ctrl
RIP1i
kDa
pSTAT1
STAT1
β-actin
85
85
45
pSTAT1 (Fold Δ)
D
MFI
pSTAT3
pSTAT5
pSTAT6
E
WT
RIP1 KD/KI
% Expression
pSTAT1+
CD206+
IFNγ+
F
% FITC-Albumin+
Vehicle-treated
RIP1i-treated
Time (min)
G
% CD69+
% IFNγ+
% LFA-1+
Unstimulated
αCD3/CD28
αCD3/CD28 + Ctrl MΦ
αCD3/CD28 + RIP1i MΦ
H
18%
37%
LFA-1
% Expression (CD4+ T cells)
CD69+LFA-1+TNFα+
I
4%
19%
IFNγ
% Expression (CD8+ T cells)
CD44+GranzB+IFNγ+
J
% CD206+
PDA
Spleen
PBMC
K
% IL-10+
L
% TNFα+
M
Tumor weight (mg)
Utx
WT; Rat IgG2a
WT; αPD-1
RIP1 KD/KI; Rat IgG2a
RIP1 KD/KI; αPD-1

Figure S4, related to Figures 5 and 6: Inhibition of RIP1 upregulates STAT1 signaling and enhances macrophage immunogenicity. (A) Day 7 BMDM were treated with RIP1i or vehicle. Expression of *Tnfa*, *Nos2*, *Ifng*, *Il1b*, *Tgfb*, and *Il6* were measured at 18 hr by qPCR. **(B)** Expression of pSTAT1 was determined at 30 min by flow cytometry in BMDM treated with RIP1i or vehicle. **(C)** Expression of pSTAT1 was determined at 30 min by western blotting in BMDM in treated with RIP1i or vehicle. Representative gel images and quantitative analysis based on densitometry are shown (n=3). **(D)** Expression of pSTAT3, pSTAT5, pSTAT6 were determined at 30 minutes by flow cytometry in BMDM were treated with RIP1i or vehicle. Quantitative data depicting median fluorescent indices (MFI) are shown. **(E)** BMDM from WT and RIP1 KD/KI mice tested for expression of pSTAT1, CD206, and IFNγ. **(F)** BMDM were treated with RIP1i or vehicle and tested for uptake of FITC-Albumin at various time points. **(G)** T cell expression of CD69, IFNγ, and LFA-1 was determined at 96 hr in unstimulated or αCD3/αCD28 treated splenic T cells, cultured alone or in the presence of TAMs harvested from control or RIP1i-treated PDA-bearing mice. **(H, I)** RIP1i-treated BMDM or controls were loaded with Ovalbumin and used to stimulate Ova-restricted $CD4^+$ (OT-II) (H) and $CD8^+$ (O-TI) T cells **(I)**. T cell activation was determined by flow cytometry at 96 hr. All *in vitro* experiments were performed at least twice in replicates of 5. **(J-L)** PBMC, spleen, and PDA-infiltrating macrophages expression of CD206 (J), IL-10 **(K)**, and TNFα **(L)** in WT mice bearing orthotopic KPC-derived tumor cells and serially administered RIP1i or fed control chow. This experiment was repeated twice. **(M)** Tumor weights on day 21 in WT mice orthotopically implanted with KPC-derived tumor cells alone, tumor cells admixed with WT BMDM, or tumor cells admixed with RIP1 KD/KI BMDM (n=5/group). Cohorts from each group were additionally treated with αPD-1. Data are displayed as average ± SEM (*$p<0.05$; **$p<0.01$; ***$p<0.001$; ****$p<0.0001$).

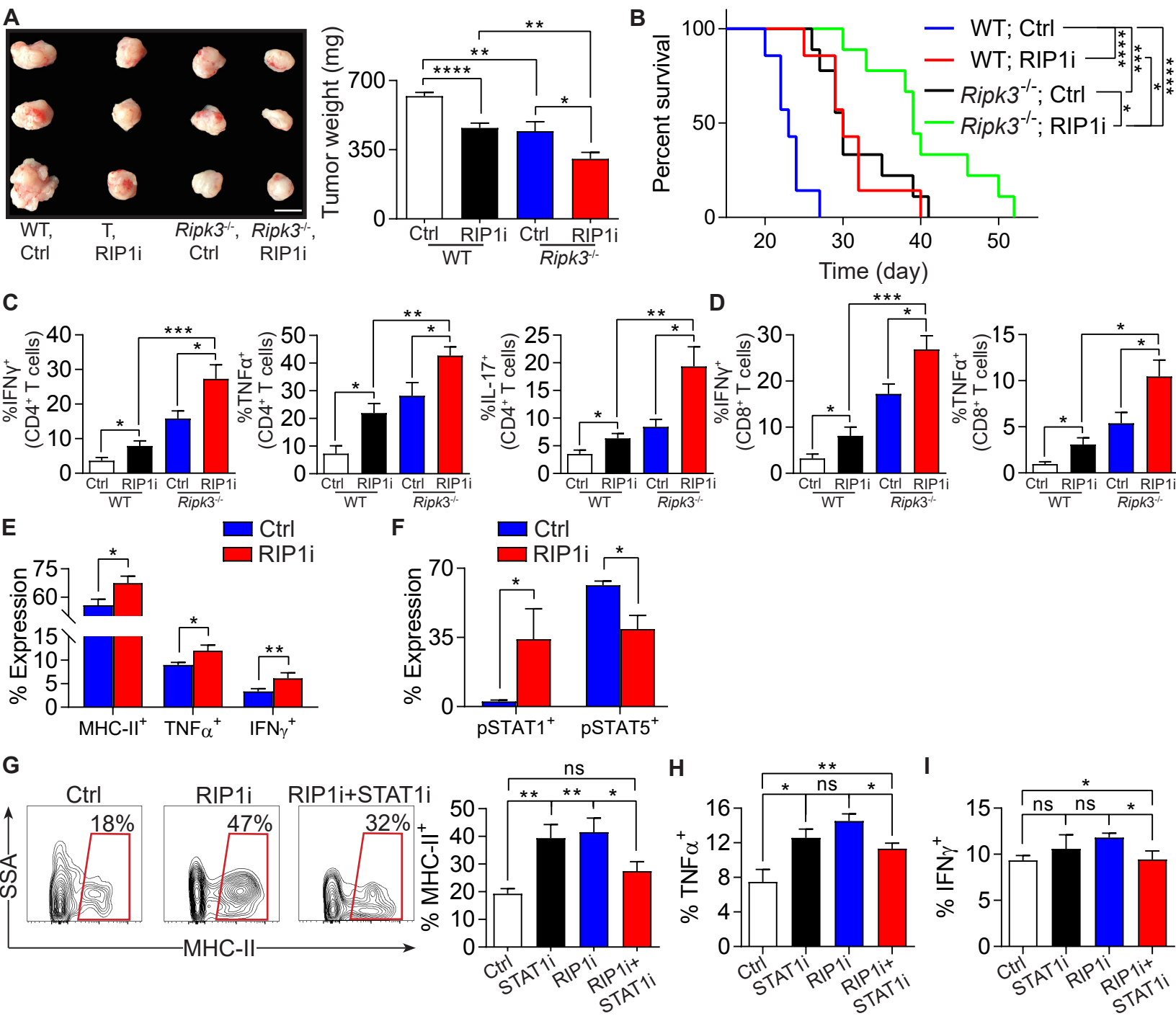
A
WT, Ctrl
T, RIP1i
Ripk3-/-, Ctrl
Ripk3-/-, RIP1i
Tumor weight (mg)
Ctrl
RIP1i
WT
Ripk3-/-
B
Percent survival
Time (day)
WT; Ctrl
WT; RIP1i
Ripk3-/-; Ctrl
Ripk3-/-; RIP1i
C
%IFNγ+ (CD4+ T cells)
%TNFα+ (CD4+ T cells)
%IL-17+ (CD4+ T cells)
D
%IFNγ+ (CD8+ T cells)
%TNFα+ (CD8+ T cells)
E
Ctrl
RIP1i
% Expression
MHC-II+
TNFα+
IFNγ+
F
pSTAT1+
pSTAT5+
G
Ctrl
RIP1i
RIP1i+STAT1i
18%
47%
32%
SSA
MHC-II
% MHC-II+
STAT1i
H
% TNFα+
I
% IFNγ+
ns

Figure S5, related to Figure 8: Tumor protective and immunogenic effects of inhibiting RIP1 are independent of RIP3. (A) Representative images (scale bar = 1 cm) and tumor weights of WT and *Ripk3*$^{-/-}$ mice bearing day 21 orthotopic KPC tumor treated with RIP1i or control (n=5/group). **(B)** Survival in cohorts of WT (n=7) and *Ripk3*$^{-/-}$ (n=9) mice bearing orthotopic KPC tumor treated with RIP1i or control was quantified with the Kaplan-Meier estimator. **(C)** Expression of IFNγ, TNFα, and IL-17 in tumor-infiltrating CD4^{+} T cells in WT and *Ripk3*$^{-/-}$ mice bearing day 21 orthotopic KPC tumor treated with RIP1i or control (n=5/group). **(D)** Expression of IFNγ and TNFα in tumor-infiltrating CD8^{+} T cells in day 21 WT and *Ripk3*$^{-/-}$ mice bearing orthotopic KPC tumor treated with RIP1i or control (n=5/group). **(E, F)** Day 7 *Ripk3*$^{-/-}$ BMDM was treated with vehicle or RIP1i and tested for expression of MHC-II, TNFα, IFNγ (E), pSTAT1, and pSTAT5 **(F)**. **(G-I)** Day 7 *Ripk3*$^{-/-}$ BMDM was treated with vehicle, RIP1i, STAT1i, or RIP1i + STAT1i and tested for expression of MHC-II (G), TNFα **(H)**, and IFNγ **(I)**. All experiments were repeated at least twice with similar results (*p<0.05; **p<0.01; ***p<0.001; ****p<0.0001). Data are displayed as average ± SEM.

Table S5, related to STAR Methods: Primer sequences for real-time PCR.

Genes	Forward primer (5'-3')	Reverse primer (5'-3')
Il1b	TCGCTCAGGGTCACAAGAAA	CATCAGAGGCAAGGAGGAAAAC
Il6	ACAAGTCGGAGGCTTAATTACACAT	TTGCCATTGCACAACTCTTTTC
Pparg	GATGCACTGCCTATGAGCAC	TCTTCCATCACGGAGAGGTC
Tgfb	CAACCCAGGTCCTTCCTAAA	GGAGAGCCCTGGATACCAAC
Tnfa	AGGCTGCCCCGACTACGT	GACTTTCTCCTGGTATGAGATAGCAAA
Nos2	GTTCTCAGCCCAACAATACAAGA	CACTGTAGCTGGGCAGGTG
Ifng	TAGCCAAGACTGTGATTGCGG	AGACATCTCCTCCCATCAGCAG
Rps6ka2	TCCTCTGGGAAATGAACAGG	TGAGAGGGACAGGCTATGCT
Ripk1	CCTGCTGGAGAAGACAGACC	CATCATCTTCCCCTCTTCCA